JOURNAL OF VIROLOGY, Nov. 1994, p. 7516–7524
0022-538X/94/$04.00+0

Vol. 68, No. 11

A Point Mutation in the *env* Gene of a Murine Leukemia Virus Induces Syncytium Formation and Neurologic Disease

BEN HO PARK,[1] BEATA MATUSCHKE,[1] EHUD LAVI,[2] AND GLEN N. GAULTON[1]*

Department of Pathology and Laboratory Medicine, Division of Immunobiology,[1] and Division of Neuropathology,[2] University of Pennsylvania, Philadelphia, Pennsylvania 19104

Received 21 April 1994/Accepted 10 August 1994

TR1.3 is a Friend-related murine leukemia virus that has been shown to cause intracerebral hemorrhages and neurologic disease due to infection and subsequent cytopathology of cerebral vessel endothelium. A striking feature of this pathology is the formation of endothelial cell syncytia. The pathogenesis of this disease has now been mapped to a single amino acid substitution of tryptophan to glycine in the variable region of the envelope protein. This same mutation enabled TR1.3 to form syncytia and retard cell proliferation in vitro in the SC-1 mouse embryoblast line but did not affect the pH dependence of viral entry. These results demonstrate that subtle molecular changes in retroviral *env* genes can induce both syncytium formation and overt clinical disease.

A prominent feature of degenerative cellular changes induced by enveloped viruses is the formation of multinucleated giant cells or syncytia. Syncytium formation occurs when the outer membranes of two or more cells fuse together to form one contiguous cell body. In the case of virally mediated fusion, it is known that viral envelope proteins mediate this process, presumably through interaction with viral envelope protein receptors on an adjacent cell (27). The consequences of virally induced syncytium formation are unclear. In some instances, the ability to induce syncytium formation has been associated with viral virulence. Recent studies have demonstrated that the onset of AIDS after human immunodeficiency virus type 1 (HIV-1) infection correlates with the emergence of HIV-1 virions that are capable of inducing syncytia (7). Although the role of syncytium formation in disease pathogenesis is still not fully known, syncytium formation has been postulated to be an important component of retrovirus-induced cell death (7, 30). These observations have increased interest in the molecular mechanisms of retrovirus-induced cell-to-cell fusion.

Murine retroviruses are useful tools for studying the molecular and cellular factors that regulate retroviral pathogenesis and, in particular, syncytium formation (11). Syncytium formation has been induced in vitro by murine leukemia viruses (MuLV) in conjunction with protease or amphotericin B treatment, and in certain transformed cell lines (4, 21, 30). However, the relevance of these observations to cellular pathology in vivo is unclear, as none of these viruses induce syncytium formation in vivo. We describe here a retroviral model of in vitro syncytium formation that accurately reflects cellular pathology and disease in vivo.

TR1.3 MuLV is a Friend-related virus that has previously been shown to induce syncytium formation of cerebral vessel endothelial cells in vivo (18). TR1.3 is selectively tropic for vessel endothelial cells and induces degenerative changes to these cells within the brain. These cellular changes initiate a cascade of pathologic processes that lead to intracerebral hemorrhages, thrombosis, infarction, and central nervous system (CNS) disease (19). Although other neurovirulent and nonneurovirulent MuLV have been reported to infect brain capillary endothelial cells (CEC), none of these MuLV induce pathologic changes in brain CEC (29).

Recombinant viruses and site-directed mutagenesis were used in this study to elucidate the viral determinants that are responsible for the unique pathogenicity of TR1.3 MuLV. In addition, an in vitro model of pathogenesis was established to determine both the mechanisms that regulate cell-to-cell fusion and how these processes affect or initiate disease. Characterization of this model revealed several similarities between TR1.3 and HIV-1-induced syncytium formation and cytopathology. These results demonstrate that the same genetic determinants regulate both syncytium formation and disease pathogenesis with TR1.3 and that these events are distinct from the events of in vitro syncytium formation as previously described for other murine retroviruses.

MATERIALS AND METHODS

Viruses and cells. Derivations of the molecular clones FB29 and TR1.3 and of recombinant viruses R3.5 and R4.3 have been described previously (18). In brief, FB29 and TR1.3 are one-long terminal repeat-permuted viral DNAs that were cloned in the same orientation in the modified vector pUC19B. Recombinant viruses R3.5 and R4.3 were constructed by reciprocally exchanging the *Sph*I-*Asc*I fragments of FB29 and TR1.3. All recombinant viruses used in this study were constructed by using standard molecular biology techniques (23). All enzymes were obtained from New England Biolabs (Beverly, Mass.). Recombinant viruses R1.9 and R2.8 were constructed by exchanging the *Sph*I-*Cla*I fragments of FB29 and TR1.3. Viruses R5.4 and R6.1 were created by exchanging the *Sph*I-*Cla*I fragments of the previously cloned R3.5 and R4.3 viruses. Viruses R9.4 and R10.3 were constructed by ligating the *Bsa*AI-*Cla*I and *Bst*1107I-*Cla*I fragments of TR1.3, respectively, into the FB29 background digested with the corresponding enzymes. Recombinant virus R11.1 was constructed by ligating the *Bst*1107I-*Cla*I fragment of FB29 into the R9.4 background digested with the same enzymes. The structure of each recombinant virus was verified by restriction enzyme digestion analysis using sites unique to either FB29 or TR1.3.

* Corresponding author. Mailing address: 422 Curie Blvd., 545 Clinical Research Building, The University of Pennsylvania School of Medicine, Philadelphia, PA 19104-6142. Phone: (215) 898-2874. Fax: (215) 573-2028.

Viral DNA was propagated in *Escherichia coli* XL-1 Blue (Stratagene, La Jolla, Calif.).

Site-directed mutants were created by using a two-step PCR process as previously described, with *Pfu* (Stratagene) for the thermostabile polymerase and plasmid FB29 (10) as the template. Outer primers used for the reaction were 5′-TATACC GTCCTACTGACTACCC-3′ (sense) and 5′-TTAGAGGTG AGATTGTTGTC-3′ (antisense). Mutagenic primers used in this study were as follows: L20I, 5′-CGGGACCTCATAATC CCCTT-3′ (sense) and 5′-AAGGGGATTATGAGGTCCCG-3′ (antisense); V80I, 5′-AGCGGGAACATTGCAGGCTG-3′ (sense) and 5′-CAGCCTGCAATGTTCCCGCT-3′ (antisense); and W102G, 5′-AACACTGCCGGGAACAGACT-3′ (sense) and 5′-AGTCTGTTCCCGGCAGTGTT-3′ (antisense) (introduced mutations are underlined). All PCRs consisted of 2 min at 94°C, followed by 45 cycles of 94°C for 30 s, 60°C for 1 min, and 72°C for 2 min. PCR products were digested with *Bsa*AI and *Bst*1107I and ligated into the FB29 background, using the Double Geneclean procedure (Bio 101, La Jolla, Calif.). The G102W mutant was created with the same PCR strategy, using the L20I virus as the template and the V80I mutagenic primers. This PCR product was ligated into the TR1.3 background at the *Bsa*AI and *Bst*1107I sites. Introduced mutations, correct fragment orientation, and absence of unwanted mutations were confirmed by sequence analysis of the entire *Bsa*AI-*Bst*1107I fragment after ligation into the FB29 or TR1.3 background, using a Sequenase sequencing kit (United States Biochemical, Cleveland, Ohio).

Infectious virus was produced by gel isolation of the permuted viruses from pUC19B after digestion with *Hin*dIII as described previously (18). Virus was then circularized with T4 DNA ligase and transfected into the feral mouse embryoblast cell line SC-1 (American Type Culture Collection, Rockville, Md.), using a modified calcium phosphate transfection procedure as described previously (28). After 10 days in culture, supernatants were harvested and assayed for the presence of reverse transcriptase (RT) (9). Viral supernatants were aliquoted and stored at −80°C. Viral titers were determined by a modified XC cell plaque assay (22). SC-1 cells were grown in minimal essential medium supplemented with 10% fetal calf serum and 1% penicillin and streptomycin. Transfected SC-1 cells were photographed with Hoffman optics after 10 days in culture.

Mice and inoculations. Virus-free pregnant female BALB/c mice were obtained from Charles River (Wilmington, Mass.). Mice were monitored daily for birth of litters. Newborn litters were used within the first 24 h after birth for inoculations. Mice were maintained on standard laboratory food and water ad libitum. Neonates were injected intracerebrally with 0.03 ml of viral supernatants within the first 24 h after birth. Control mice were inoculated with an equal volume of supernatant from mock-transfected SC-1 cells. Mice were monitored daily for symptoms of tremor, seizure, and paralysis. Mice were inoculated with equivalent amounts of virus as assessed by RT activity and XC plaque assays, with titers ranging from 4×10^4 to 5×10^6 PFU/ml.

Antibodies and lectin. Purified polyclonal goat anti-Rauscher gp70 was obtained from the Biological Carcinogenesis Branch of the National Cancer Institute (Bethesda, Md.). Fluorescein-conjugated monoclonal rat anti-goat immunoglobulin G was purchased from Fisher Scientific (Pittsburgh, Pa.). Rhodamine-conjugated BS-1 lectin was purchased from Sigma Chemical Co. (St. Louis, Mo.).

Immunohistochemical analyses. Frozen tissue sections were prepared from brains of 2-week-old mice that had been inoculated with virus or from brains of age-matched mock-infected controls. Serial sections 6 μm thick were fixed with methanol for 2 min at −20°C and then incubated with normal sheep serum (2% in 20 mM sodium phosphate [pH 7.4]–150 mM sodium chloride [phosphate-buffered saline {PBS}]) for 20 min at 4°C. Sections were then incubated with primary antibodies after which fluorescein- and rhodamine-conjugated secondary reagents were added for 30 min at 4°C. Three washes in PBS were performed on each section between incubations. Goat anti-Rauscher gp70 antibody and fluorescein-conjugated rat anti-goat immunoglobulin G were used at final concentrations of 95 and 5 μg/ml, respectively. Rhodamine-conjugated BS-1 lectin was used at a final concentration of 50 μg/ml. Sections were analyzed, and fluorescence intensity was quantified with a Nikon Optiphot fluorescence microscope.

Histopathological analyses. Tissue samples from brains were taken from symptomatic mice that were inoculated with neuropathogenic viruses or from age-matched infected controls. Organs were fixed in formalin and embedded in paraffin, and serial sections were prepared for hemotoxylin and eosin staining.

Quantification of syncytia in SC-1 cell cultures. TR1.3-transfected, FB29-transfected, and untransfected SC-1 cells were seeded in T-75 flasks and grown to confluence. Percentages of syncytia were calculated by dividing the total number of syncytia by the number of counted fields. A total of 1,012 fields were counted twice for each cell line, using a Lovins microslide field finder (Teledyne Gurley, Troy, N.Y.).

[^{3}H]thymidine incorporation assays. Incorporation assays were performed as previously described (15). In brief, 5×10^2 cells were plated in 96-well flat-bottom plates and were pulsed with [^{3}H]thymidine (1 μCi per well) for 6 h after 24, 48, 72, and 96 h in culture. Cells were harvested with a PHD harvester (Cambridge Technology Inc., Cambridge, Mass.) and counted in a liquid scintillation counter.

Effects of lysosomotropic agents on viral entry. SC-1 cultures were plated in 24-well culture plates (10^4 cells per well) and incubated overnight. The following morning, cultures were placed on ice and incubated with 10-fold dilutions of TR1.3 or FB29 viral supernatant for 1 to 2 h to allow virus binding to SC-1 cells. Chloroquine (50 and 100 μM) or ammonium chloride (50 and 100 mM) was then added to the wells, and the cultures were incubated at 37°C for 3 to 12 h. In some experiments, lysosomotropic agents were added to cultures with virus at 4°C. Prewarmed medium was used in place of lysosomotropic agents as a control in all experiments. After various incubation times, cells were washed five times with medium, refed fresh medium, and allowed to incubate at 37°C for 36 h. Viral supernatants were harvested and used to quantify infection by using the RT assay as described above. TR1.3 and FB29 chronically infected cell lines were treated in an identical manner to control for nonspecific protein inhibition by lysosomotropic agents. RT activity was quantified with a PhosphorImager (Molecular Dynamics, Sunnyvale Calif.).

Fusion assays. SC-1 cells transfected with TR1.3 and FB29 and untransfected SC-1 cells were seeded into six-well plates (5×10^4 cells per well) and allowed to attach overnight at 37°C for 12 h. Medium was removed and replaced with medium supplemented with 50 mM morpholineethanesulfonic acid (MES) and 50 mM *N*-2-hydroxyethylpiperazine-*N*′-2-ethanesulfonic acid (HEPES) adjusted to pH 5.0, 6.0, 7.0, or 8.0 with HCl or NaOH. Cells were exposed to these conditions for 30 s, 1 min, 3 min, 5 min, 1 h, 6 h, or 12 h. After pH treatment, uninfected SC-1 cells were overlaid, and syncytium formation was assessed at 12, 24, and 36 h.

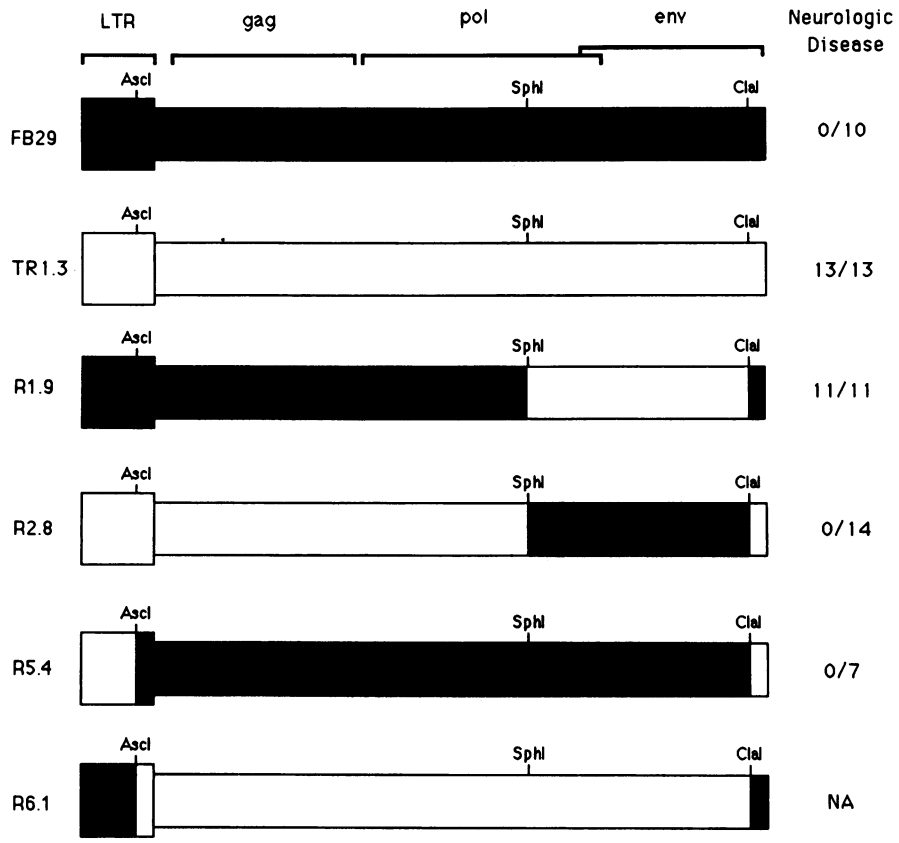

FIG. 1. The *Sph*I-*Cla*I fragment harbors the determinants for inducing CNS disease. Recombinant viral DNA genomes were constructed by using TR1.3 MuLV and FB29 Friend MuLV as described in Materials and Methods. Infectious viruses derived from these DNA constructs were used to inoculate neonatal BALB/c mice. Mice were monitored daily for symptoms of neurologic disease. Results are pooled from three separate experiments. LTR, long terminal repeat; NA, not applicable.

RESULTS

The envelope gene of TR1.3 is responsible for neuropathogenicity and in vivo syncytium formation. Previous studies using recombinant viruses constructed with the neuropathogenic TR1.3 and the nonneuropathogenic Friend MuLV, FB29 (25), demonstrated that the genetic determinants responsible for inducing syncytium formation in vivo reside within a 3.0-kb *Sph*I-*Asc*I fragment of TR1.3 that contained the 3′ end of *pol* and the majority of the *env* gene (18). Additional recombinant viruses were constructed to more precisely map these neuropathogenic determinants. As seen in Fig. 1, the capacity of TR1.3 to induce syncytia and subsequent CNS disease mapped to the *env* gene. Initial recombinants were constructed by reciprocal substitution of the *env* region to produce viruses R1.9 and R2.8 and by reciprocal substitution of the U3 region of the long terminal repeat to produce viruses R5.4 and R6.1. Transfection of these viral DNAs produced infectious virus within 10 to 14 days in tissue culture. Infectious virus could not be produced from recombinant R6.1 or an identical, independently derived clone, R6.2, despite repeated attempts. Infectious virions of parental FB29 and TR1.3 and of recombinants R1.9, R2.8, and R5.4 were then inoculated into neonatal BALB/c mice. As shown in Fig. 1, only mice infected with TR1.3 and R1.9 developed neurologic disease. Disease was characterized by tremor, seizure activity, and eventually paralysis at 11 to 13 days postinoculation. This was accompanied by intracerebral hemorrhage, thrombosis, and infarction, identical to findings previously reported for the parental TR1.3 virus (19). As shown in Fig. 2A and B, the most distinctive pathologic feature of mice infected with R1.9 was syncytium formation of cerebral vessel endothelial cells. Pathologic changes were not found in mice infected with R2.8 or R5.4 virus; however, the levels of viral protein expression in endothelial cells appeared to be identical for all viruses. As shown in Fig. 2C and D, the brains of R1.9- and R2.8-infected animals displayed levels of immunofluorescence staining equivalent to that of the gp70 envelope protein, as quantified by microfluorimetry. Double-fluorescence staining using anti-gp70 antibody and BS-1, a lectin that recognizes murine endothelium, confirmed that viral protein expression was specific for vessel endothelial cells as previously described (18).

A second panel of recombinant viruses was constructed to further map the region of TR1.3 that confers the pathogenic phenotype. The envelope gene of TR1.3 was first dissected into a 600-bp *Bsa*AI-*Bst*1107I fragment and a 1,400-bp *Bst*1107I-*Cla*I fragment. As shown in Fig. 3, these fragments were cloned individually and concurrently into the FB29 background to yield viruses R9.4, R10.3, and R11.1. Infectious virus from these plasmid DNA was used to inoculate neonatal BALB/c mice. Mice infected with the R9.4 and R11.1 viruses developed neurologic disease identical to that seen in TR1.3-infected mice within 10 to 13 days postinoculation. In contrast, mice infected with R10.3 did not exhibit any neurodegenerative

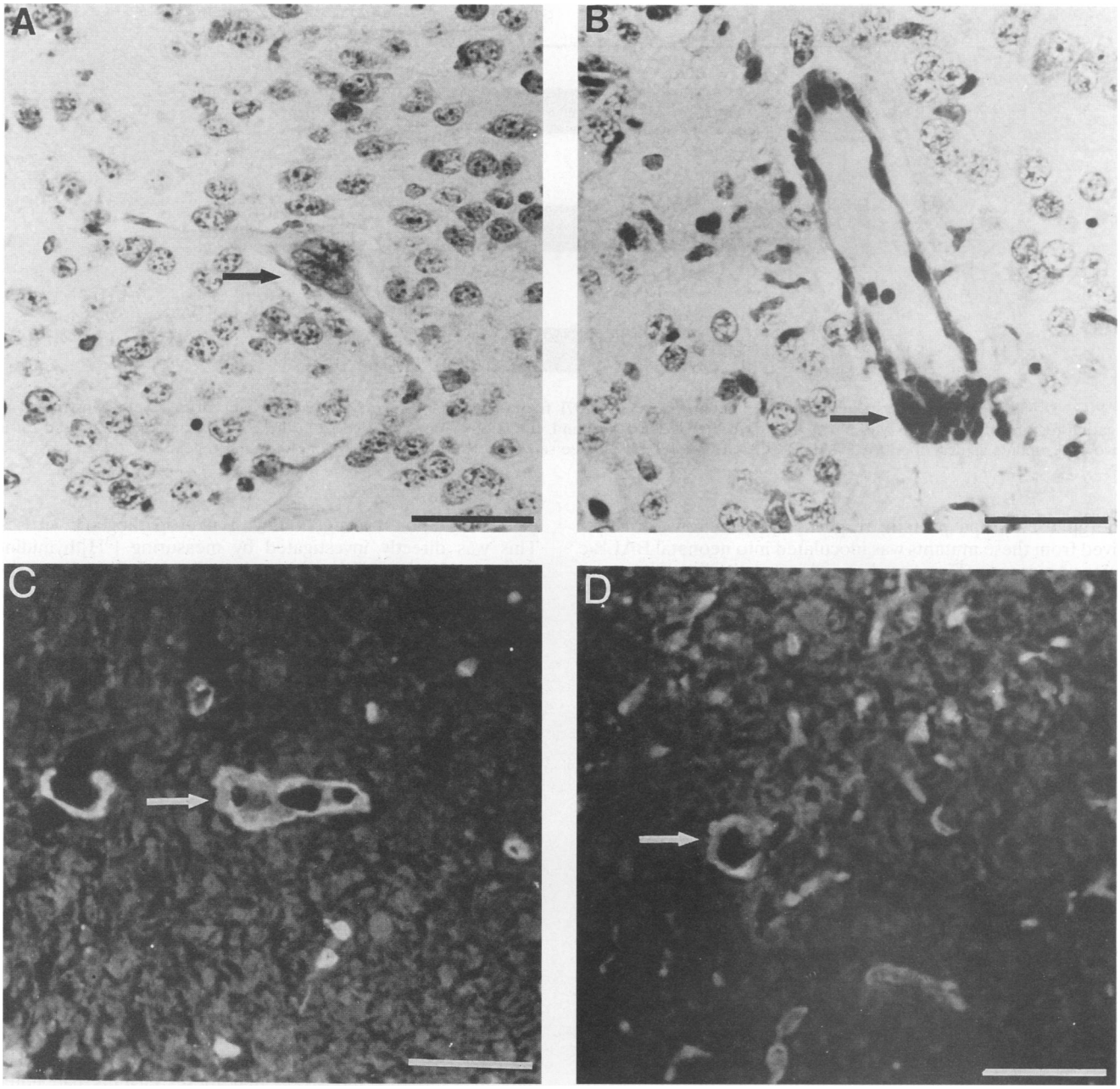

FIG. 2. Neuropathogenic recombinant viruses infect and induce syncytium formation of brain endothelial cells in vivo. (A and B) Histologic analysis of brains from symptomatic R1.9-infected BALB/c mice. Syncytia of small vessel endothelial cells are shown (arrows). (C and D) Immunohistochemical analysis of anti-gp70 antibody binding. The staining of endothelial cells in brain sections from mice inoculated with R1.9 (C) and R2.8 (D) viruses is shown (arrows). Bars = 100 μm.

symptoms. Histopathology and immunohistochemical analysis confirmed that while each of these viruses displayed envelope protein expression in vessel endothelium, syncytia of cerebral vessel endothelia and other CNS pathology were seen only in mice infected with recombinant viruses R9.4 and R11.1. These data demonstrate that the molecular determinants that regulate syncytium formation and CNS disease reside within a 600-bp region in the 5′ end of the envelope gene.

A point mutation within the envelope gene is responsible for the syncytium formation of cerebral endothelial cells and CNS disease. To further elucidate the mechanisms that mediate the neuropathogenicity of TR1.3, the 600-bp *Bsa*AI-*Bst*1107I fragment of TR1.3 was sequenced and compared with the published sequence of FB29 (20). As shown in Table 1, three nucleotide differences that affected amino acid changes were detected within this fragment. Site-directed mutagenesis was performed at each of these sites within FB29 MuLV in an attempt to convert the nonpathogenic phenotype to the neurovirulent phenotype of TR1.3. Three mutants were generated that produced single amino acid substitutions of leucine to isoleucine, valine to isoleucine, and tryptophan to glycine at position 20 of the leader peptide and positions 80 and 102 of

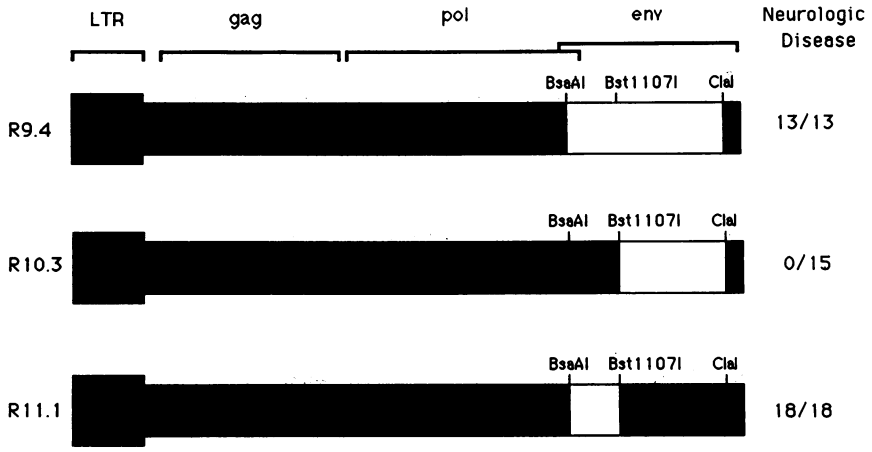

FIG. 3. Neuropathogenicity resides within a 600-bp *Bsa*AI-*Bst*1107I fragment of TR1.3 MuLV. Recombinant viruses were constructed by ligating regions of the TR1.3 MuLV *env* gene into the FB29 background. Infectious virus produced from these DNA constructs was used for in vivo experiments as described for Fig. 1. Results are pooled from three separate experiments. LTR, long terminal repeat.

the gp70 envelope protein, respectively. Infectious virus derived from these mutants was inoculated into neonatal BALB/c mice. As seen in Fig. 4, only mice infected with the mutant W102G developed neurologic disease. Disease incidence, symptoms, and CNS pathology were identical to those seen with TR1.3-induced disease. Immunohistochemical analysis indicated that mice infected with all three viruses displayed equivalent levels of viral protein within vessel endothelial cells; however, the presence of multinucleated endothelial giant cells was detected only in W102G-inoculated mice. The reciprocal point mutation of W102G, termed G102W, was constructed in an attempt to abrogate the neuropathogenicity of TR1.3 MuLV. The G102W virus differed from the parental TR1.3 virus only at amino acid 102 of the envelope protein, containing a tryptophan-for-glycine substitution at this position. Infectious virus could not be produced from this molecular clone or an identical independently derived clone, G102W.2, despite repeated attempts.

In vivo syncytium formation and CNS disease correlate with in vitro syncytium formation and reduced cellular proliferation. Viruses used throughout this study were propagated in vitro on the wild mouse embryoblast cell line SC-1. SC-1 cells are normally not permissive for syncytium formation by MuLV. However, transfection of SC-1 cell cultures with the neuropathogenic viruses TR1.3, R1.9, R9.4, R11.1, and W102G resulted in a dramatic increase in the number of multinucleated giant cells in vitro. Transfection with the nonneuropathogenic viruses FB29, R2.8, R5.4, R10.3, L20I, and V80I did not result in increased syncytium formation of SC-1 cell cultures. As shown in Fig. 5A, SC-1 cells transfected with the W102G virus formed multinucleated cells typically consisting of 3 to 12 nuclei. As displayed in Fig. 5B, SC-1 cells transfected with nonneuropathogenic virus (L20I) or mock-transfected controls showed no change in the level of multinucleated cells. Multinucleated giant cells were occasionally found in mock-transfected SC-1 cells at very low frequency. The proportion of multinucleated giant cells found in SC-1 cell cultures transfected with neuropathogenic virus was 74.0% (Fig. 5C). In comparison, the frequencies of syncytia observed in mock-transfected SC-1 cells and those transfected with nonneuropathogenic viruses were 0.7 and 0.6%, respectively.

The marked difference in SC-1 cell density shown in Fig. 5A and B also suggested that the growth kinetics of SC-1 cells were decreased upon transfection with neuropathogenic viruses. This was directly investigated by measuring [^{3}H]thymidine incorporation of SC-1 cells that were seeded at the same density and assayed at 24 to 96 h after transfection. As shown in Fig. 5D, TR1.3-transfected SC-1 cells displayed decreased [^{3}H]thymidine incorporation compared with FB29-transfected or mock-transfected cells. Slower growth and decreased [^{3}H]thymidine incorporation were observed in all cultures transfected with neuropathogenic viruses used in this study. Cells transfected with nonneuropathogenic viruses displayed growth rates equal to those of mock-transfected controls.

TR1.3 and FB29 viral entry have identical pH requirements. The capacity of many enveloped viruses to induce syncytium formation at neutral pH has been correlated with a pH-independent route of viral entry. The entry of MuLV into SC-1 cells has been previously reported to be dependent on an acidic endosomal pathway (3). The relationship between the mechanisms of viral entry and syncytium formation utilized by the pathogenic TR1.3 and the nonpathogenic FB29 MuLV was investigated by comparing the pH requirements for these two processes. SC-1 cells were exposed to TR1.3 and FB29 MuLV in the presence of the lysosomotropic agent chloroquine or ammonium chloride, and infection was detected by RT activity after 36 h. These drugs were previously shown to block MuLV entry into SC-1 cells by raising the pH of endosomes (3). The data in Table 2 demonstrate that these reagents had equal effects on the inhibition of both TR1.3 and FB29 entry into SC-1 cells. SC-1 cells chronically infected with TR1.3 and FB29 were used as controls for nonselective inhibitory effects of

TABLE 1. Amino acid differences between TR1.3 and FB29 envelope proteins within the *Bsa*AI-*Bst*1107I fragment

Amino acid no.[a]	Amino acid	
	TR1.3	FB29
20	Ile	Leu
80	Ile	Val
102	Gly	Trp

[a] 20 represents the 20th amino acid of the 34-amino-acid leader peptide. 80 and 102 represent the 80th and 102nd amino acids, respectively, within the gp70 envelope protein.

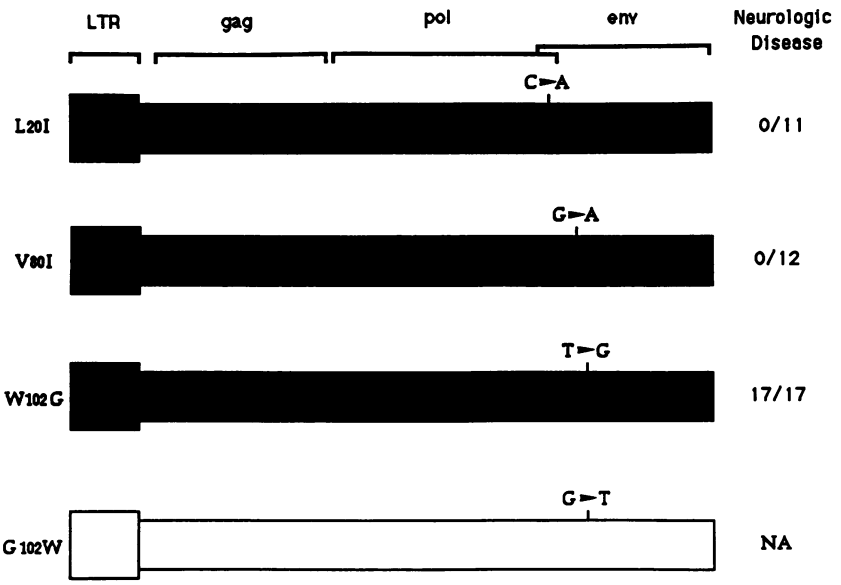

FIG. 4. A tryptophan-to-glycine amino acid substitution is responsible for in vivo syncytium formation and CNS disease. Single point mutations were introduced into FB29 Friend MuLV at the nucleotide bases shown above the 5′ *env* region. These mutations resulted in amino acid substitutions at position 20 of the leader peptide (L20I) and positions 80 and 102 of the gp70 envelope protein (V80I and W102G, respectively). A single point mutation was also created in the TR1.3 MuLV shown in the indicated region above the 5′ *env* gene (G102W). Infectious virus was produced from these DNA constructs and used for in vivo experiments as described for Fig. 1. Results are pooled from three separate experiments. LTR, long terminal repeat; NA, not applicable.

these agents on the production of RT, such as decreased protein synthesis. The data in Table 2 demonstrate that RT production in these chronically infected cell lines was inhibited only at 100 mM ammonium chloride.

The effect of pH on the ability of TR1.3 and FB29 to form syncytia is also shown in Table 2. The number of multinucleated giant cells in TR1.3- and FB29-infected cultures was not affected by the pH of the culture medium over a range of pH 5.0 to 8.0. These results demonstrate that the pH fusion requirements for TR1.3 viral entry and syncytium formation are regulated by independent processes.

DISCUSSION

The capacity of TR1.3 MuLV to induce CNS disease and syncytium formation has been mapped to a single point mutation within the amino terminus of the envelope protein, using recombinant viruses and site-directed mutagenesis. Other MuLV have also been shown to harbor determinants of neurologic disease within the 5′ region of *env* (8, 14, 17, 26). These MuLV infect brain CEC but induce spongiform encephalopathies without pathologic changes to brain CEC. The role of endothelial cells in mediating these spongiform changes remains unclear. The neurovirulence of one MuLV, *ts*1, has been mapped to a single amino acid substitution of isoleucine for valine at amino acid 25 of the envelope precursor protein gPr80^{env} (26). This mutation results in inefficient processing and sequestration of gPr80^{env} within the endoplasmic reticulum of primary cultures of astrocytes but not endothelial cells, although both cell types are infected (24). The Friend MuLV PVC-211 also causes a spongiform encephalopathy similar to that caused by *ts*1, yet does not demonstrate inefficient processing of the gPr80^{env} precursor protein (14). PVC-211 does not infect astrocytes but selectively infects brain CEC without inducing pathologic changes to these cells.

The pathogenesis of disease induced by TR1.3 is distinct from that induced by other neuropathogenic MuLV. TR1.3 infection of endothelial cells appears to be directly linked to the final process of CNS disease, since degenerative endothelial cell changes were always associated with cerebral vascular pathology following infection with TR1.3, R1.9, R9.4, R11.1, and W102G viruses. Therefore, while it is likely that multiple overlapping pathways account for the formation of MuLV-dependent spongiform encephalopathies, TR1.3-associated neurologic disease is caused by a single mechanism that compromises the integrity of brain CEC.

The neuropathogenicity of TR1.3 directly correlated with the ability to induce syncytia in vivo and in vitro. The mechanism of TR1.3-induced syncytium formation is not fully known. MuLV virions can, under some circumstances, induce syncytium formation in vitro. Virus-mediated cell-to-cell fusion or syncytium formation has been shown to occur by two methods: a single virion can fuse two or more cells simultaneously (fusion from without), or virally infected cells expressing envelope proteins can fuse directly with each other (fusion from within). Current theory suggests that syncytium formation is a consequence of a shift in the pH dependency of the events involved in viral envelope-mediated fusion. Viruses that fuse with cells at the plasma membrane utilize a pH-independent mechanism. Syncytium formation by these viruses is not affected by pH. Viruses that fuse with the cell membrane only within an acidic endosome require a low pH for entry. These viruses cannot induce cell to cell fusion until they encounter an acidic environment, as has been shown for influenza and Semliki Forest viruses (27).

Recent evidence suggests that the regulation of retroviral fusion is more complex, as the correlation between syncytium formation and a pH-independent route of viral entry is not always observed. For example, Wilson et al. demonstrated that a strain of Moloney MuLV was capable of inducing syncytia in

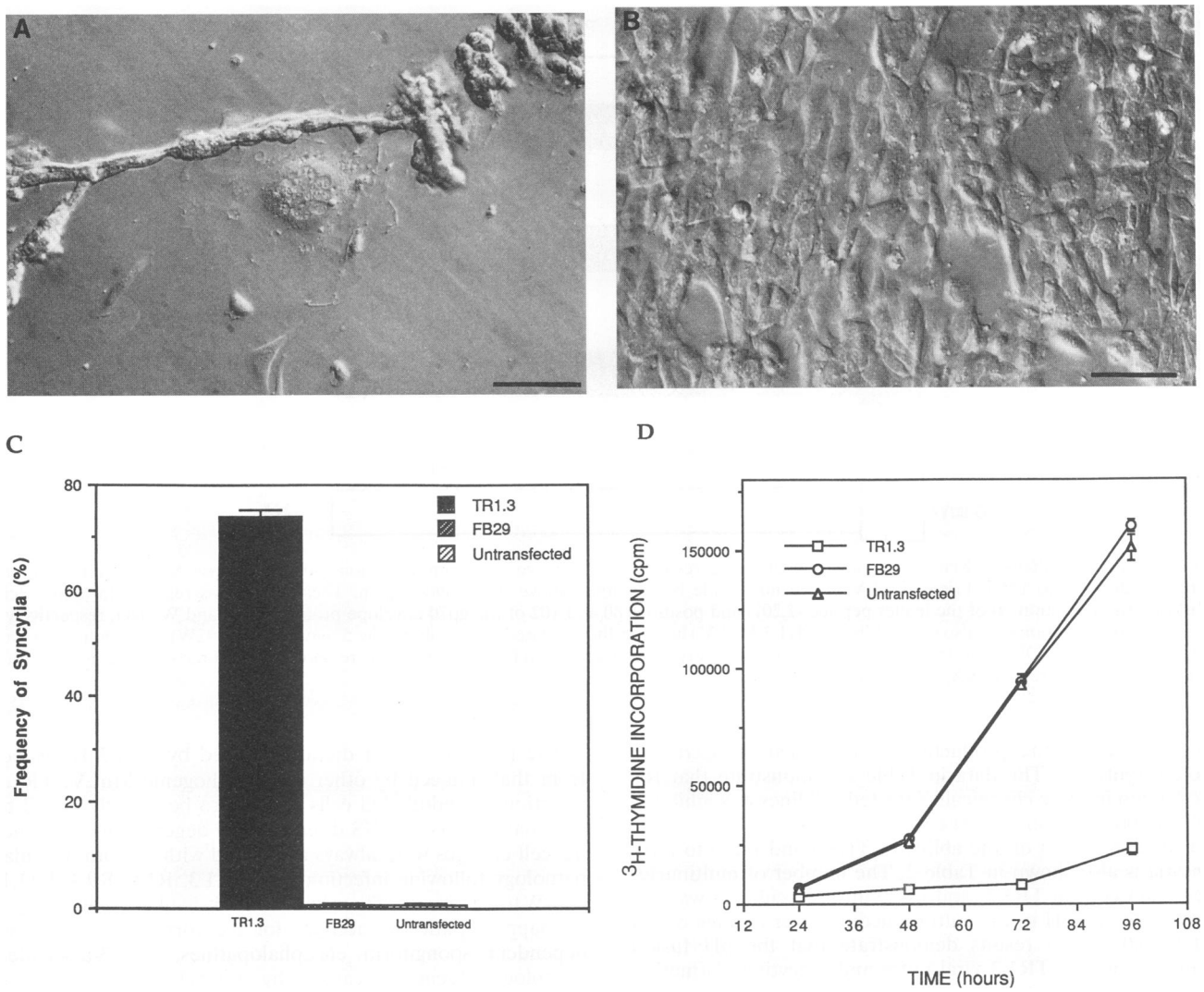

FIG. 5. Neuropathogenic MuLV-induced syncytia and slowed growth of SC-1 cells. Neuropathogenicity in vivo was compared with cytopathicity in vitro, using the SC-1 embryoblast cell line. (A and B) Photomicrographs of SC-1 cells transfected with neuropathogenic W102G (A) and nonneuropathogenic L20I (B) viruses after 10 days in culture. Both cultures were initially seeded at 5×10^5 cells per ml. Bars = 100 μm. (C) Frequency of multinucleated giant cells in SC-1 cultures transfected with TR1.3, FB29, and no DNA. The level of syncytium formation was quantified as described in Materials and Methods. Results are pooled from duplicate samples and represent the mean and the standard error of the mean. (D) [^{3}H]thymidine incorporation of SC-1 cells transfected with TR1.3, FB29, or no DNA was performed at 6-h intervals over the time course shown. Results are pooled from triplicate samples. Each datum point represents the mean value ± the standard error of the mean.

a *ras*-transformed NIH 3T3 cell line at neutral pH but still required a low-pH-dependent route of viral entry (30). In addition, several lines of evidence suggest that HIV-1-mediated viral entry and syncytium formation may utilize different fusion mechanisms (12). The data presented here are in agreement with these observations. TR1.3-induced syncytium formation was not affected by pH; however, TR1.3 required the same pH-dependent mechanism(s) of viral entry as the non-syncytium-inducing FB29 MuLV. The results suggest that the fusion pH requirements for TR1.3 viral entry versus syncytium formation are distinct.

Battini et al. (6) have shown that the amino terminus of envelope surface (SU) proteins contains two regions of variability, which they designated VRA and VRB. The VRA region is the major determinant of receptor specificity. Our sequence analysis demonstrates that the tryptophan-to-glycine substitution that is responsible for the syncytium-inducing phenotype of TR1.3 lies within the VRA segment of envelope. Furthermore, this trytophan residue is highly conserved among different molecular clones of Friend MuLV. In contrast, the genetic determinants responsible for in vitro syncytium formation by other MuLV have been shown to reside within the amino-terminal portion of the p15E transmembrane (TM) envelope protein (11). Syncytium formation by these MuLV has never been correlated with virulence in vivo. It is possible that fusion events are regulated by multiple mechanisms and that fusion related to viral entry and nonpathologic syncytium formation is affected by the TM envelope subunit, while fusion related to pathologic syncytium formation is mediated by the variable region of the SU envelope glycoprotein.

A similar situation has been demonstrated for HIV-induced syncytium formation. The TM protein gp41 has been impli-

TABLE 2. pH requirements for TR1.3 viral entry and syncytium formation are distinct[a]

Virus	Viral entry			Syncytium formation assay	
	Lysosomotropic agent	% Inhibition of RT activity (mean ± SE)			
		Acutely infected	Chronically infected	pH of medium	Synctium formation[b]
TR1.3	Chloroquine, 50 μM	81 ± 1	0[c]	5.0	+
	Chloroquine, 100 μM	84 ± 5	0[c]	6.0	+
	NH_4Cl, 50 mM	89 ± 2	0[c]	7.0	+
	NH_4Cl, 100 mM	92 ± 2	89 ± 6	8.0	+
FB29	Chloroquine, 50 μM	84 ± 4	0[c]	5.0	−
	Chloroquine, 100 μM	89 ± 4	0[c]	6.0	−
	NH_4Cl, 50 mM	91 ± 5	9 ± 1[c]	7.0	−
	NH_4Cl, 100 mM	92 ± 4	28 ± 18	8.0	−

[a] Results are representative of six separate experiments.
[b] + and − denote syncytium formation greater than 50% and less than 1%, respectively, using the quantification criteria described in the legend to Fig. 5.
[c] Results are statistically significant by Student's t test ($P < 0.001$).

cated in HIV-induced fusion; however, sequence analysis of virions isolated from HIV-1 infected patients demonstrate that the syncytium-inducing versus non-syncytium-inducing phenotype is due to mutations within the hypervariable regions of the SU protein, gp120 (5). It is, therefore, possible that amino acid changes within the variable regions of retroviral SU glycoproteins mediate syncytium formation that is a prelude to disease, while TM proteins mediate fusion involved with viral entry, as well as syncytium formation in vitro that may or may not be related to disease.

The data presented here do not suggest a definitive mechanism for how the tryptophan-to-glycine substitution in the gp70 SU protein enables virus-induced cell-cell fusion to occur. Several models can be proposed on the basis of the current literature. This amino acid change may create a proteolytic cleavage site that enables cell surface proteases to alter the gp70 molecular conformation and induce fusion. Alternatively, this change may alter the affinity of envelope-receptor interactions, thus allowing syncytium formation to occur by virtue of prolonged exposure between membranes. This latter mechanism has recently been shown to account for syncytium formation induced by a parainfluenza virus (16). These two mechanisms are not mutually exclusive, and neither necessitates that the route of viral entry be affected concomitant with the ability to induce syncytia. These hypotheses may also explain the selective degenerative effect of TR1.3 on brain endothelium. Cerebral vascular endothelium is known to contain unique enzymes that may cleave the viral envelope protein as a result of the presence of a unique protease-sensitive site on TR1.3, and/or the tight junctions that are present only in brain CEC may allow prolonged exposure between two juxtaposed cells, thus enabling the membranes to fuse. Studies are presently under way to evaluate these processes in TR1.3 directed fusion.

A decrease in cellular growth and [^{3}H]thymidine incorporation was seen in SC-1 cultures transfected with neuropathogenic MuLV used in this study. Other retroviruses have also shown similar kinds of cytopathic effect in vitro, including HIV *env*-transfected cell lines (2). Decreased [^{3}H]thymidine incorporation could be due to a decrease in cellular proliferation and/or an increase in cell death, possibly due to syncytium formation. Further studies are currently being performed to assess the mechanisms and consequences of growth retardation induced by TR1.3.

The inability to produce infectious virus from recombinant viral DNA of R6.1 and G102W is not unprecedented. Similar results are reported for several retroviruses, including HIV-1 chimeric DNA (1). It is possible that lethal mutations were inadvertently introduced into recombinant viral genomes during the cloning process, thereby preventing the production of mature virions. This explanation does not seem probable with R6.1 and G102W because additional independently derived and sequenced clones, R6.2 and G102W.2, also failed to produce infectious virus. In addition, infectious virions were produced from R2.8 and another previously reported recombinant virus, R4.3, that contained the *env* and U3 region of FB29 in the TR1.3 background. These results suggest that there are unique features within retroviral genomes that cannot be substituted with homologous genomic regions. These data also imply that genome-specific *cis*-acting regulatory motifs may be involved in MuLV transcriptional control, since the U3 region contains consensus promoter/enhancer elements for transcriptional binding factors (13). Further recombinant viruses are presently being constructed to test this hypothesis and gain insight into this perplexing issue.

The data presented in this study show that the *env* region of TR1.3 MuLV is responsible for the cytopathic effects that lead to CNS disease. This phenomenon is regulated by a single amino acid substitution of tryptophan to glycine at position 102 in the variable region of the gp70 envelope protein. This mutation does not, however, alter the pH dependence of viral entry. Further analysis of TR1.3 MuLV provides a means to address how genetic changes affect syncytium formation in a pathophysiologic system and may ultimately reveal the molecular pathways involved in retrovirus-induced cytopathology.

ACKNOWLEDGMENTS

We thank Avinash Bhandoola, Dave Levy, and Dave Weiner for technical assistance and advice.

B.H.P. is a scholar of the Life and Health Insurance Medical Research Fund. G.N.G. is a Scholar of the Leukemia Society of America. This work was supported by grant PO1-NS30606.

REFERENCES

1. **Adadchi, A., H. E. Gendelman, S. Koenig, T. Folks, R. Willey, A. Rabson, and M. A. Martin.** 1986. Production of acquired immunodeficiency syndrome-associated retrovirus in human and nonhuman cells transfected with an infectious molecular clone. J. Virol. **59**:284–291.
2. **Ahmad, A., A. Ladha, E. A. Cohen, and J. Menezes.** 1993. Stable expression of the transfected HIV-1 *env* gene in a human B cell line: characterization of gp120-expressing clones and immunobiological studies. Virology **192**:447–457.

3. **Andersen, K. B., and B. A. Nexø.** 1983. Entry of murine retrovirus into mouse fibroblasts. Virology **125:**85–98.
4. **Andersen, K. B., and H. Skov.** 1989. Retrovirus-induced cell fusion is enhanced by protease treatment. J. Gen. Virol. **70:**1921–1927.
5. **Andeweg, A. C., M. Groenink, P. Leeflang, R. E. Y. de Goede, A. D. M. E. Osterhaus, M. Tersmette, and M. L. Bosch.** 1992. Genetic and functional analysis of a set of HIV-1 envelope genes obtained from biological clones with varying syncytium-inducing capacities. AIDS Res. Hum. Retroviruses **8:**1803–1813.
6. **Battini, J., J. M. Heard, and O. Danos.** 1992. Receptor choice determinants in the envelope glycoproteins of amphotropic, xenotropic, and polytropic murine leukemia viruses. J. Virol. **66:**1468–1475.
7. **Cheng-Mayer, C., D. Seto, M. Tateno, and J. A. Levy.** 1988. Biologic features of HIV-1 that correlate with virulence in the host. Science **240:**80–82.
8. **Gardner, M. B.** 1985. Retroviral spongiform polioencephalomyelopathy. Rev. Infect. Dis. **7:**99–110.
9. **Goff, S., P. Traktman, and D. Baltimore.** 1981. Isolation and properties of Moloney murine leukemia virus mutants. Use of a rapid assay for the release of virion reverse transcriptase. J. Virol. **38:**238–248.
10. **Ho, S. N., H. D. Hunt, R. M. Horton, J. K. Pullen, and L. R. Pense.** 1989. Site-directed mutagenesis by overlap extension using the polymerase chain reaction. Gene **77:**51–54.
11. **Jones, J. S., and R. Risser.** 1993. Cell fusion induced by the murine leukemia virus envelope glycoprotein. J. Virol. **67:**67–74.
12. **Larsen, C., H. Ellens, and J. Bentz.** 1992. Membrane fusion induced by the HIV *env* glycoprotein, p. 143–166. *In* R. C. Aloia, C. C. Curtain, and L. M. Gordon (ed.), Membrane interactions of HIV. Wiley-Liss, Inc., New York.
13. **Manley, N. R., M. A. O'Connell, P. A. Sharp, and N. Hopkins.** 1989. Nuclear factors that bind to the enhancer region of nondefective Friend murine leukemia virus. J. Virol. **63:**4210–4223.
14. **Masuda, M., M. P. Remington, P. M. Hoffman, and S. K. Ruscetti.** 1992. Molecular characterization of a neuropathogenic and nonerythroleukemogenic variant of Friend murine leukemia virus PVC-211. J. Virol. **66:**2798–2806.
15. **Merida, I., P. Williamson, W. A. Kuziel, W. C. Greene, and G. N. Gaulton.** 1993. The serine-rich cytoplasmic domain of the interleukin-2 receptor-β chain is essential for interleukin-2-dependent tyrosine protein kinase and phosphatidylinositol-3-kinase activation. J. Biol. Chem. **268:**6765–6770.
16. **Moscona, A., and R. W. Peluso.** 1993. Relative affinity of the human parainfluenza virus type 3 hemagglutinin-neuraminidase for sialic acid correlates with virus-induced fusion activity. J. Virol. **67:**6463–6468.
17. **Paquette, Y., Z. Hanna, P. Savard, R. Brousseau, Y. Robitaille, and P. Jolicoeur.** 1989. Retrovirus-induced murine motor neuron disease: mapping the determinant of spongiform degeneration within the envelope gene. Proc. Natl. Acad. Sci. USA **86:**3896–3900.
18. **Park, B. H., E. Lavi, K. J. Blank, and G. N. Gaulton.** 1993. Intracerebral hemorrhages and syncytium formation induced by endothelial cell infection with a murine leukemia virus. J. Virol. **67:**6015–6024.
19. **Park, B. H., E. Lavi, A. Stieber, and G. N. Gaulton.** 1994. Pathogenesis of cerebral infarction and hemorrhage induced by a murine leukemia virus. Lab. Invest. **71:**78–85.
20. **Perryman, S., J. Nishio, and B. Chesebro.** 1991. Complete nucleotide sequence of Friend murine leukemia virus strain FB29. Nucleic Acids Res. **19:**6950.
21. **Pinter, A., T. Chen, A. Lowy, N. G. Cortez, and S. Silagi.** 1986. Ecotropic murine leukemia virus-induced fusion of murine cells. J. Virol. **57:**1048–1054.
22. **Rowe, W. P., W. E. Pugh, and J. W. Hartley.** 1970. Plaque assay techniques for murine leukemia viruses. Virology **42:**1136–1139.
23. **Sambrook, J., E. F. Fritsch, and T. Maniatis.** 1989. Molecular cloning: a laboratory manual, 2nd ed. Cold Spring Harbor Laboratory, Cold Spring Harbor, N.Y.
24. **Shikova, E., Y. C. Lin, K. Saha, B. R. Brooks, and P. K. Y. Wong.** 1993. Correlation of specific virus-astrocyte interactions and cytopathic effects induced by *ts*1, a neurovirulent mutant of Moloney murine leukemia virus. J. Virol. **67:**1137–1147.
25. **Sitbon, M., B. Sola, L. Evans, J. Nishio, S. F. Hayes, K. Nathanson, C. F. Garon, and B. Chesebro.** 1986. Hemolytic anemia and erythroleukemia, two distinct pathogenic effects of Friend MuLV: mapping of the effects to different regions of the viral genome. Cell **47:**851–859.
26. **Szurek, P. F., P. H. Yuen, J. K. Ball, and P. K. Y. Wong.** 1990. A Val-25-to-Ile substitution in the envelope precursor polyprotein $gPr80^{env}$, is responsible for the temperature sensitivity, inefficient processing of $gPr80^{env}$, and neurovirulence of *ts*1, a mutant of Moloney murine leukemia virus TB. J. Virol. **64:**467–475.
27. **White, J. M.** 1992. Membrane fusion. Science **258:**917–924.
28. **Wigler, M., A. Pellicer, S. Silverstein, R. Axel, G. Urlaub, and L. Chasin.** 1979. DNA-mediated transfer of the adenine phosphoribosyltransferase locus into mammalian cells. Proc. Natl. Acad. Sci. USA **76:**1373–1376.
29. **Wiley, C. A., and M. Gardner.** 1993. The pathogenesis of murine retroviral infection of the central nervous system. Brain Pathol. **3:**123–128.
30. **Wilson, C. A., J. W. Marsh, and M. V. Eiden.** 1992. The requirements for viral entry differ from those for virally induced syncytium formation in NIH 3T3/DTras cells exposed to Moloney murine leukemia virus. J. Virol. **66:**7262–7269.